

## Supporting Information

# Deep learning-based denoising for improved dose efficiency in EDX tomography of nanoparticles

*Alexander Skorikov,<sup>a,b</sup> Wouter Heyvaert,<sup>a,b</sup> Wiebke Albrecht,<sup>a,b</sup> Daniël M. Pelt<sup>c</sup>*

*and Sara Bals<sup>\*a,b</sup>*

<sup>a</sup>EMAT, University of Antwerp, Groenenborgerlaan 171, 2020 Antwerp, Belgium

<sup>b</sup>NANOLab Center of Excellence, University of Antwerp, Groenenborgerlaan 171, 2020 Antwerp, Belgium

<sup>c</sup>Leiden Institute of Advanced Computer Science, Niels Bohrweg 1, 2333 CA Leiden, The Netherlands

\*To whom all correspondence should be addressed: sara.bals@uantwerpen.be

### Original noisy simulated EDX maps

In this work we studied denoising of extremely noisy EDX maps, which corresponds to low acquisition times and electron illumination doses in experiments. Unfortunately, when displaying such maps directly, the distribution of the signal becomes essentially invisible because of high amounts of noise. For this reason, the visibility of noisy simulated EDX maps in the main text of the paper was enhanced by applying a  $3\times 3$  uniform filter. In Figure S1 and Figure S2 we provide the original versions for the noisy maps shown in the main text.

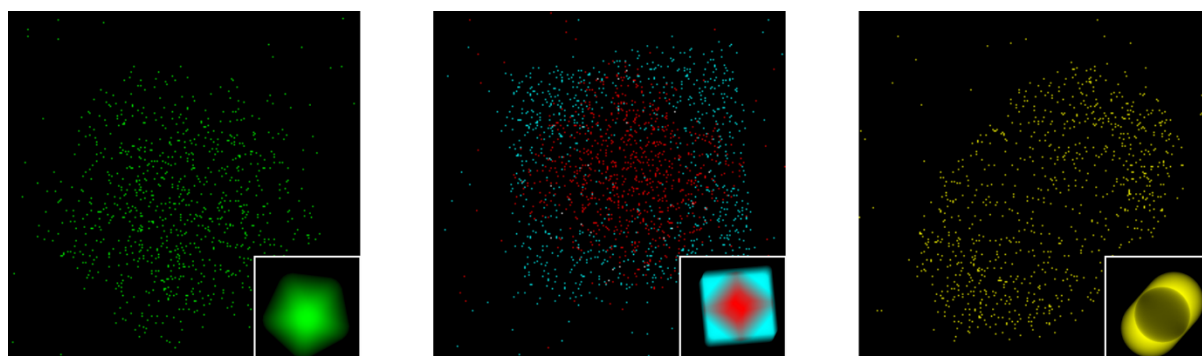


**Figure S1.** Original, noisy versions of simulated EDX maps displayed in Figure 1 in the main text of the paper. Insets show reference clean data.

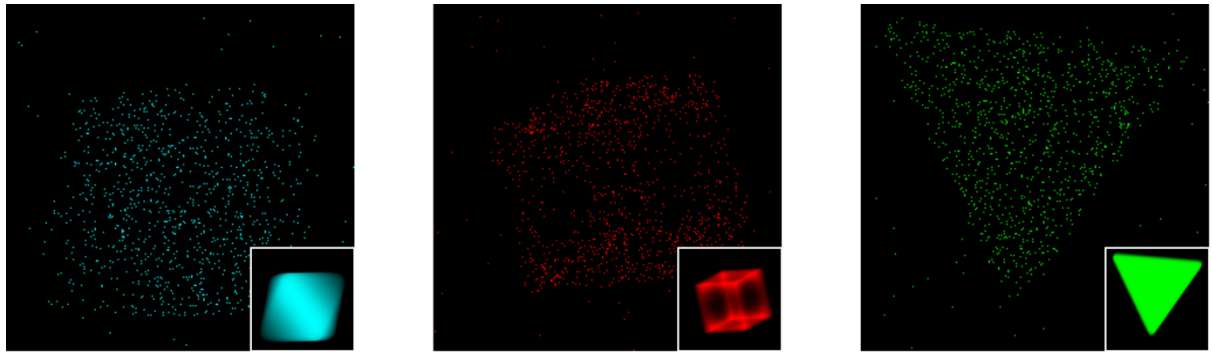


**Figure S2.** Original, noisy versions of simulated EDX maps displayed in Figure 2 in the main text of the paper. Insets show reference clean data.

### Verification of EDX noise model

To verify that only taking into account the Poisson distribution of signal realistically conveys the noise features expected for EDX data, we studied the relationship between the mean value  $\mu$  and the variance  $\sigma^2$  of the signal in experimental EDX elemental maps. From **Figure S3** it can be seen that this relationship perfectly follows the  $\mu = \sigma^2$  dependency expected for the Poisson distribution. This shows the absence of *e.g.* additive noise in experimental data and indicates that the Poisson distribution adequately captures the statistical properties of the experimental EDX signal.

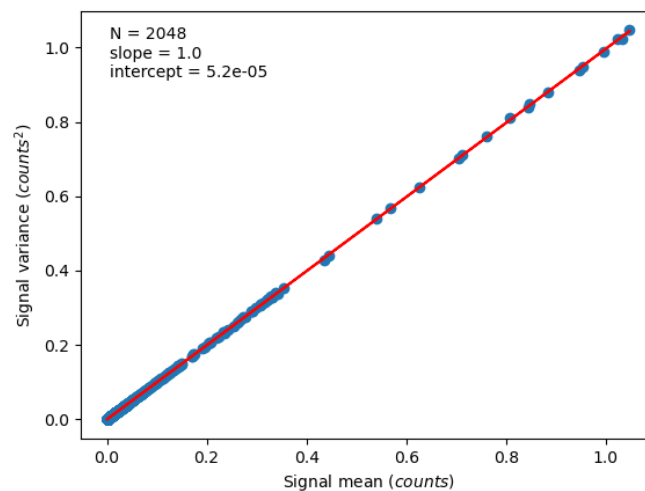


**Figure S3.** Relationship between the signal mean and variance for a set of 2048 experimental EDX elemental maps indicating Poisson distribution of EDX signal. Data points represent individual elemental maps, and the red line depicts a linear least-squares fit of the data.

## Comparison of 2D and 3D denoising

To compare whether it is better to denoise 2D projection images before performing the 3D reconstruction or applying the denoising in 3D after the reconstruction, we performed numerical experiments based on simulated data and the Gaussian denoising method. Gaussian denoising was chosen because it is computationally inexpensive in both 2D and 3D, whereas the qualitative outcome of the comparison is expected to hold for TV and U-net based denoising. The test was performed on 150 data points from the generated database by comparing the normalized mean absolute error between the reference structure and the 3D reconstruction obtained using the respective denoising methods. The parameters of the denoising algorithm (Gaussian sigma) for each data point were chosen by numerically minimizing the total absolute error between the denoised data and the reference tilt series (in 2D case) or the reference 3D structure (for 3D denoising). **Figure S4a** shows that 2D based denoising significantly outperforms the 3D approach. An example of a qualitative comparison between the best reconstructions of a generated particle obtained using the respective methods are displayed in Figure S4b-e.

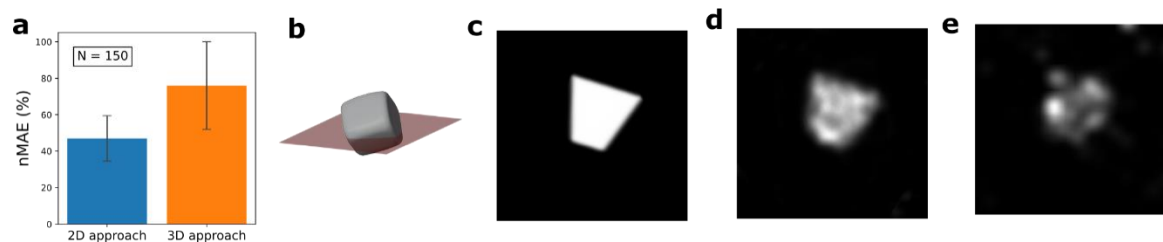


**Figure S4.** (a) Quantitative comparison of 3D reconstruction quality using 2D and 3D signal denoising approaches on a set of 150 simulated particles. (b-e) Example of the denoising results for both methods. Visualization of (b) 3D shape and (c) position of the slice through a generated particle. Slices through the best quality reconstructions using (d) 2D and (e) 3D denoising approaches.

One explanation for the better performance of 2D based denoising is that the 3D reconstruction of noisy data by maximum likelihood algorithms (such as EM or SIRT) introduces additional

artifacts because of overfitting to noise in the input data. Conversely, denoising the data before the reconstruction allows the algorithm to converge to a more sensible estimate of the 3D structure.

### Neural network architecture

In this work, we used a well-known U-net network architecture, which contains a series of  $3 \times 3$  convolution operations followed by  $2 \times 2$  max pooling in the encoder path, followed by a symmetric series of  $2 \times 2$  up-convolutions in the decoder. At each stage of upsampling, features from the encoder path are combined with the previous layer output from the decoder path to aid high-resolution feature localization. The final layer of the network is a  $1 \times 1$  convolution resulting in the denoised 2D image. In this work, zero-padding of 1 pixel was used in all convolution operations to preserve the size of the image after denoising.

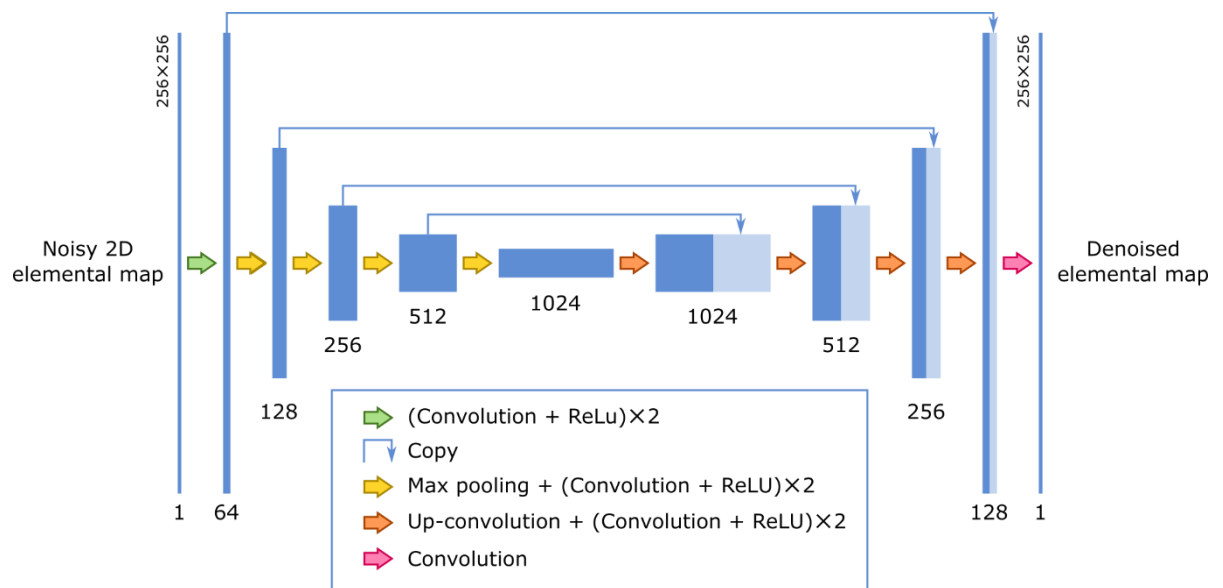


**Figure S5.** Schematic illustration of the U-net architecture used for the deep learning-based denoising in this work.